Solid State Ionics 324 (2018) 226–232

Contents lists available at ScienceDirect

Solid State Ionics

journal homepage: www.elsevier.com/locate/ssi

Characterization of thin film $Li_{0.5}La_{0.5}Ti_{1-x}Al_xO_3$ electrolyte for all-solid-state Li-ion batteries

Seda Ulusoy[a], Sena Gulen[a], Gulnur Aygun[a], Lutfi Ozyuzer[a,b], Mehtap Ozdemir[a,b,*]

[a] Department of Physics, Izmir Institute of Technology, 35430 Urla, Izmir, Turkey
[b] Teknoma Technological Materials Inc., Izmir Institute of Technology Campus, 35430 Urla, Izmir, Turkey

ARTICLE INFO

Keywords:
Ionic conductivity
$Li_{0.5}La_{0.5}Ti_{1-x}Al_xO_3$
Solid electrolyte
Magnetron sputtering

ABSTRACT

Since addition of Al in $Li_{0.5}La_{0.5}TiO_3$ has enhanced ionic conductivity in bulk materials, it is important to apply this material on all solid state thin film batteries. Because some of the good ionic conductors such as Lithium Phosphorus Oxynitride (LiPON) are sensitive to oxygen and moisture and their application is limited, so amorphous $Li_{0.5}La_{0.5}Ti_{1-x}Al_xO_3$ (LLTAlO) is a most promising candidate because of its stability. In this study, the crystalline LLTAlO targets were prepared changing the amount of x content by conventional solid state reactions. Using these targets, lithium lanthanum titanium oxide (LLTO) thin film electrolytes were deposited on ITO/SLG substrates by radio frequency magnetron sputtering system in Ar atmosphere. The structural and compositional properties of targets and thin films were characterized by SEM, XRD, Raman spectroscopy and XPS. It was found that all targets are crystalline while the thin films are amorphous. To understand the effect of Al doping on ionic conductivity, electrical measurements were done at room temperature by AC impedance spectroscopy forming ITO/LLTAlO/Al structure like capacitor. Highest ionic conductivity result, 0.96×10^{-6} S·cm^{-1}, is obtained from the nominal thin film composition of $Li_{0.5}La_{0.5}Ti_{1-x}Al_xO_3$ (x = 0.05) at room temperature measurements. Heat treatment is also conducted to investigate to understand its effect on ionic conductivity and the structure of the thin films. It is found that ionic conductivity enhances with annealing. Also, temperature dependent ionic conductivity measurements from 298 K to 385 K are taken in order to evaluate activation energy for Li-ion conduction.

1. Introduction

Due to the increasing demand of energy sources, it is crucial to develop energy storage technology in a way that the environment is protected and give response to demands of today's living standards like higher energy density, longer lifespan, lightweight and flexible designs [1]. All solid state batteries have attracted much attention to bring solutions for new improvements. Commonly used liquid electrolytes have begun to fail because of some safety concerns like leakage and pollution, although they serve high ionic conductivity at room temperature [2]. On the other side, lithium ion conducting solid electrolytes have received substantial interest because of their significant advantages such as thermal stability, resistance to shocks and vibrations, and miniaturization capability [3].

Especially by the thin film applications of all solid state batteries, it is possible to provide higher volumetric and gravimetric energy densities [4,5]. Electrolyte layer, which is the main focus in this study, is responsible for the ionic conduction from anode to cathode regions during charge and discharge cycle of a battery. This phenomenon has crucial importance to determine system performance in terms of charge/discharge rate, power density and efficiency [6].

The first compound of this solid electrolyte family of $Li_{3x}La_{(2/3)-x}TiO_3$ was synthesized by Belous et al. [7] and their outstanding room temperature lithium conductivity enhanced by Inaguma et al. [8] with highest ionic conductivity 10^{-3} S/cm up to that date. Since then, much attention has been paid to ABO_3 perovskite type $Li_{3x}La_{(2/3)-x}TiO_3$ (LLTO) compound and its structurally related modifications to enhance its ionic conductivity. The reason for this high ionic conduction is explained by the presence of vacancies on A-site of the lattice which allows Li^+ to move freely through the vacant sites of the ABO_3 perovskite LLTO structure [9]. Furthermore, it is found that perovskite structure can tolerate having different valence states on A-site and B-site and this enables to develop substitutional structure modifications like Al substitution for Ti to increase ionic conductivity like in our research topic. In the study of Morata-Orrantia et al. [10], $La_{2/3}Li_xTi_{1-x}Al_xO_3$ was examined as bulk structure with compositions of x

* Corresponding author at: Department of Physics, Izmir Institute of Technology, 35430 Urla, Izmir, Turkey.
E-mail address: mehtapozdemir@teknoma.net (M. Ozdemir).

https://doi.org/10.1016/j.ssi.2018.07.005
Received 26 December 2017; Received in revised form 13 June 2018; Accepted 6 July 2018
Available online 19 July 2018

and the highest ionic conductivity was calculated as 7.6×10^{-5} S·cm^{-1} at room temperature, which proved that Al substitution have positive effect on ionic conduction up to some level. During the intercalation process, a reduction of Ti^{4+} to Ti^{3+} at low potentials causes short circuit by the electronic conduction [11]. So with the light of this knowledge, it is necessary to prevent reduction. Therefore, substitution of Al for Ti becomes our focus in this research [12]. Besides, lower effective ionic radii of Al^{3+} ($r_{Al}{}^{3+} = 0.53$ Å) compared to Ti^{4+} ($r_{Ti}{}^{4+} = 0.605$ Å) enables less reduction by Al substitution [13]. Furthermore, different composition-structure and ionic conductivity properties of LLTO were studied by Youmbi et al. [14] and found that $Li_{0.5}La_{0.5}TiO_3$ composition has the highest ionic conductivity as 1.7×10^{-3} S·cm^{-1} among $Li_{0.34}La_{0.51}TiO_{2.94}$, $Li_{0.27}La_{0.59}TiO_3$, $Li_{0.34}La_{0.56}TiO_3$ (cubic), $Li_{0.34}La_{0.56}TiO_3$ (tetragonal), $Li_{0.10}La_{0.63}TiO_3$ compositions.

As a result, $Li_{0.5}La_{0.5}TiO_3$ composition is chosen as our starting material, later by aluminum substitution $Li_{0.5}La_{0.5}Ti_{1-x}Al_xO_3$ samples were synthesized with different x compositions (x = 0.01, 0.05, 0.10, 0.15). The powders were prepared after some steps of conventional solid state reactions, and then they were pressed in a Cu-base plate in order to form a ceramic powder target for the RF magnetron sputtering process. $Li_{0.5}La_{0.5}Ti_{1-x}Al_xO_3$ (LLTAlO) thin films were grown on indium tin oxide (ITO)/Soda lime glass (SLG) substrate under pure Ar atmosphere. ITO/SLG, which were grown and improved by our group [15,16], were preferred as a substrate to obtain contact from the back side of the thin film electrolyte for the impedance measurements to determine ionic conductivities. Ionic conductivity of samples was determined using probe station. Furthermore, to explain the relationship between the ionic conduction and the structure of the thin films, SEM, XRD, Raman and XPS analysis were realized for the structural characterizations. In the present study, Al doped LLTO thin film growth is the first study according to the best of our knowledge.

2. Experimental

2.1. Target preparation

The $Li_{0.5}La_{0.5}TiO_3$ pure and doped targets were prepared by conventional solid state reaction from stoichiometric amounts of Li_2CO_3 (Sigma Aldrich, 99.997%), La_2O_3 (Sigma Aldrich, 99.999%), and TiO_2 (Sigma Aldrich, > 99.5%) powders. The batch of powders was mixed by using agate and pestle for 6 h in order to obtain homogeneous mixture for the calcination process. Then, the stoichiometric mixture of the powder was put in alumina crucible boat and calcinated 3 times at 1200 °C in air for 6 h. During these treatments CO_2 gas was released. After every step of calcination, powder was grinded. Finally, the calcinated batch was poured in a 2 inch circular Cu base plate ground and pressed with a cylindrical button at 5 MPa and sintered at 600 °C for 1 h in air to have compact and solid mass form for sputtering process. In addition, for Al doping, Al_2O_3 (Sigma Aldrich, 99.99%) powder was added to mixed powder after the second and third calcination was performed again at 1200 °C for 6 h in air [17] for various stoichiometric Al doped LLTO targets. The produced LLTO targets were placed into the sputter gun of the vacuum chamber pumped by turbomolecular pump to grow LLTO thin films using RF magnetron sputtering technique.

2.2. Thin film deposition by RF magnetron sputtering technique

Through RF-magnetron sputtering method, thin films were deposited under high vacuum on SLG and ITO/SLG substrates. The sputtering was done using the pure and Al doped LLTO targets. Before deposition, the substrates were cleaned in ultrasonic cleaner with ethyl alcohol and de-ionized water, respectively, for 5 min. When the vacuum chamber was evacuated down to low 10^{-6} Torr, 5 min pre-sputtering of LLTO and LLTAlO target, and later 60 min deposition was carried out under 50 sccm Ar atmosphere. The working gas pressure, the distance between the target and substrate, and the sputtering power were 4.78 mTorr, 13 cm, and 96 W, respectively. The film thicknesses were measured as 120 nm by profilometer. LLTO and LLTAlO films were also subjected to annealing process at temperatures 100, 200, 300, and 400 °C for 2 h in air ambient to observe the effect of annealing treatment on the structure and ionic conductivity of the solid state electrolyte.

2.3. Characterization

The crystallinity of the various composition targets and the thin films were determined by X-ray diffraction method using X'Pert Pro diffractometers with Cu K_α X-ray radiation wavelength of 1.54 Å over the angular range $20^\circ < 2\theta < 80^\circ$ with a 0.0334° step. The surface morphology of the thin films with various Al_2O_3 content was determined by scanning electron microscopy (SEM) using Philips XL 30SFEG operated at 3.0 kV using TLD detector. Confocal Raman spectroscopy setup (Scientific Instruments) with Argon laser having 488 nm excitation wavelength with 600 grating was used to determine the vibrational peaks of $Li_{0.5}La_{0.5}TiO_3$ and $Li_{0.5}La_{0.5}Ti_{1-x}Al_xO_3$ targets with various x content.

X-ray photoelectron spectroscopy (XPS) analyses were performed using a SPECS Phoibos 150 3D-DLD system with using Mg K_α radiation ($h\nu = 1254$ eV) operated at 200 W, 1.5 kV. The high resolution scans of each element in $Li_{0.5}La_{0.5}Ti_{1-x}Al_xO_3$ were conducted at 30 eV pass energy with a scan rate of 0.1 eV/s and the dwell time of 1 s. The spectra were calibrated with respect to C 1s at 284.6 eV which is the characteristic of aromatic/aliphatic carbons.

In order to evaluate ionic conductivities of the thin films on ITO/SLG, Al was evaporated on the upper side of the thin films via Leybold UNIVEX thermal evaporation device by using a shadow mask. Aim of the mask usage was to create contact areas for the ionic conductivity calculations. Janis Probe Station was used to take contacts from ITO on the back side and Al on the top. Impedance measurements were performed at controlled temperatures within the frequency range from 0.1 Hz to 200 kHz with IM 3590 HIOKI impedance analyzer.

3. Results and discussion

3.1. Characterization of the targets and $Li_{0.5}La_{0.5}Ti_{1-x}Al_xO_3$ thin films

The surface morphology and the microstructure of thin films were characterized by SEM. Fig. 1(a) shows the morphology of the ITO surfaces on SLG substrate. The image shows grain structure as seen most of the ITO studies [15]. In Fig. 1(b), the undoped LLTO film surface can be seen. It is understand that the grown films follow similar surface morphology of the underlayer ITO surface. SEM images of thin films deposited with different Al substitution were also presented in Fig. 1(c), (d), (e) and (f). It can be observed that LLTAlO thin films have also similar grain size with ITO film. It is found that the all coated surfaces have the same morphology with ITO surfaces showing that the Al substitution does not affect the morphology of the grown films on ITO.

X-ray diffraction (XRD) analysis for the crystallographic characterization of the targets and produced thin films were done to determine the perovskite LLTAlO structure. In Fig. 2, all the diffraction peaks of the targets, at $2\theta = 29.3^\circ$, 32.8°, 40.3°, 47.0°, 58.4°, 68.6° and 78.1° correspond to planes (101), (110), (112), (200), (212), (220) and (310) that can be ascribed to the reflections of $LiLaTiO_3$ crystalline phase [18], which confirms that the fabrication process conducted in this work is appropriate with those reported in related literature results [19].

The thin films of LLTO and LLTAlO deposited on ITO/SLG substrates do not show any crystalline peaks of LLTO target. Thin films are amorphous, since peaks observed in Fig. 3 belong to ITO/SLG substrate. When the peaks of ITO substrate are investigated, there is a broad peak

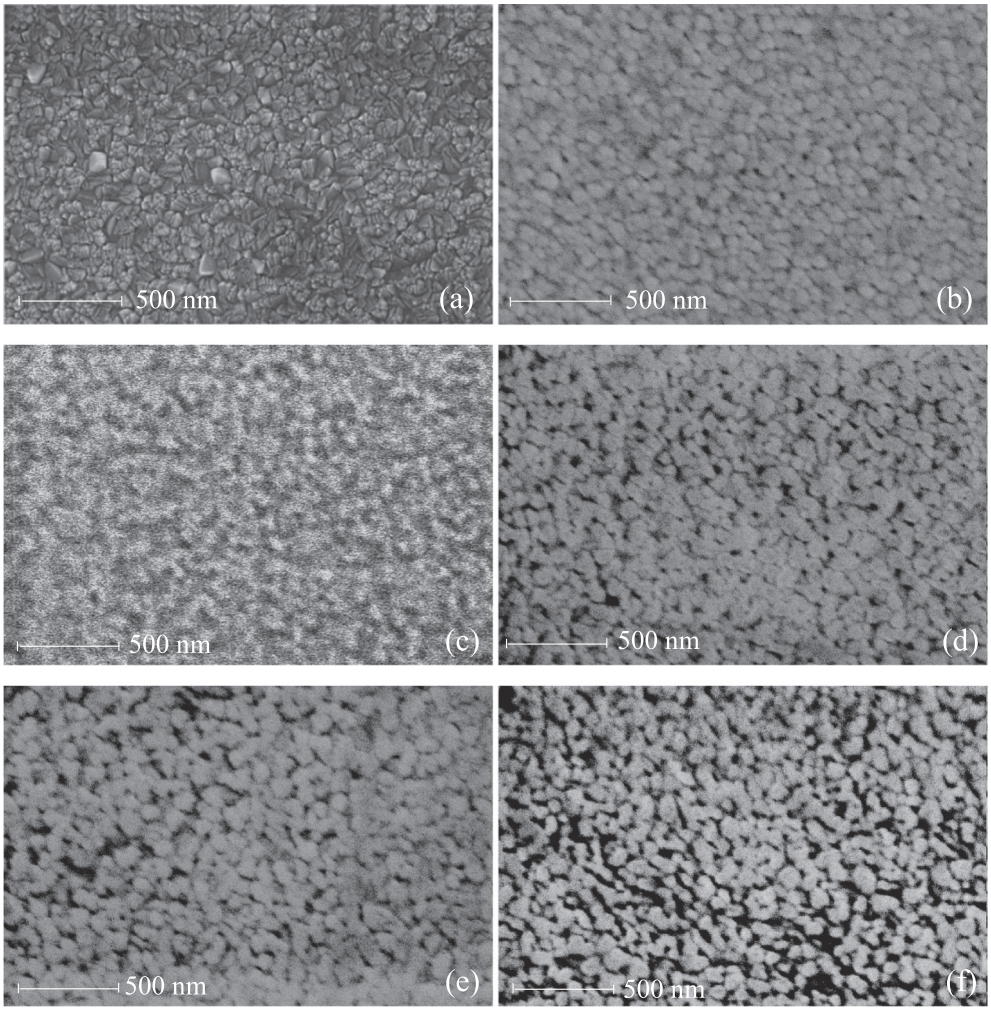

Fig. 1. SEM image of the thin film surface of $Li_{0.5}La_{0.5}Ti_{1-x}Al_xO_3$ (a) ITO coated SLG substrate (b) pure (x = 0) (c) x = 0.01 (d) x = 0.05 (e) x = 0.10 (f) x = 0.15.

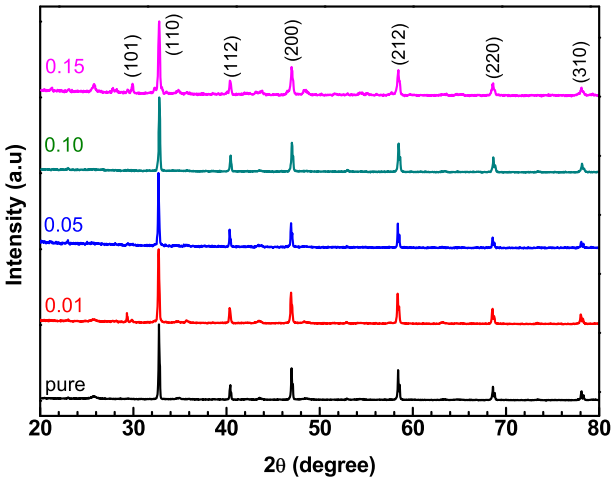

Fig. 2. XRD patterns of all $Li_{0.5}La_{0.5}Ti_{1-x}Al_xO_3$ targets, which are expressed as nominal compositions of $Li_{0.5}La_{0.5}TiO_3$ (pure), $Li_{0.5}La_{0.5}Ti_{1-x}Al_xO_3$ (x = 0.01, 0.05, 0.10, 0.15).

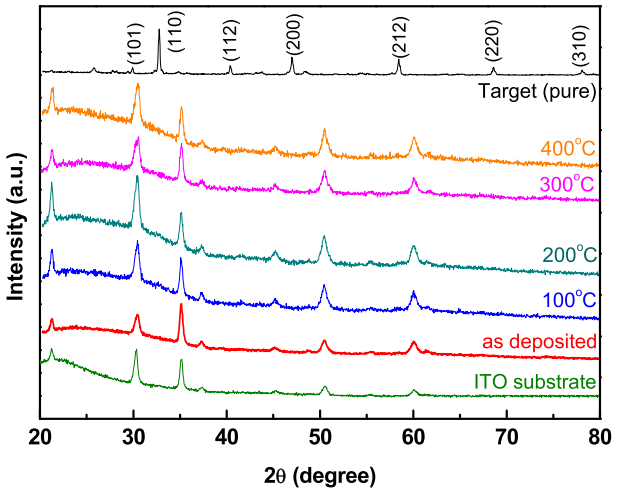

Fig. 3. XRD patterns of $Li_{0.5}La_{0.5}TiO_3$ (pure) target and films annealed in air for 2 h at 100, 200, 300 and 400 °C and the crystalline peaks of the ITO substrate.

around the 21° coming from the glass. On the other hand, the peaks coming from LLTO is around 24° and this peak is broader. Annealed films at 100, 200, 300 and 400 °C for 2 h in air atmosphere were also examined. However, they are also amorphous. Therefore, it is observed that the annealing does not have any effect on crystallization. The detailed grazing incidence XRD studies were done on the films and proved amorphous structure of the films.

Thin films after annealing maintained its amorphous structure, so its structure is independent from the annealing temperatures. Amorphous structure has beneficial aspects for the ionic conduction like promoting

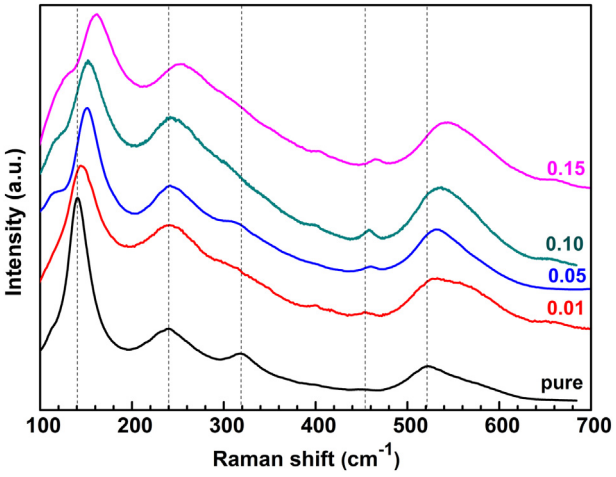

Fig. 4. Raman spectroscopy results of the targets with different Al (x) compositions.

3 dimensional conduction mechanisms. The high ionic conductivity of the amorphous thin film according to the crystalline one could be resulted from a structural disorder of the amorphous structure, an interface enhancement effect, a stress in the thin film and the absence of grain boundaries [3]. Li ion is transferred via hopping for the amorphous thin films which called as diffusion migration path along the thin film. As the amorphous structure provides 3D, open and disordered environment for the Li ion, it promotes conduction in 3D. On the other hand, amorphous thin films have lower ionic conductivity compared to single crystalline bulk that has ABO_3 perovskite type crystal structure. The advantage of thin films is that their lithium ion conductivity does not need to be as high as compared to bulk solid electrolytes, taking into account the electrolyte resistance; $R = l * (\sigma * A)^{-1}$, where A is the contact area, l is the thickness and σ is the Li-ion conductivity of the solid electrolyte, respectively. If the same compound as bulk and thin film form considered having the same resistance, their conductivities will be inversely proportional to the thickness. Therefore, it can be said that to reach high conductivity results for the thin film samples of the same compound is not needed.

Fig. 4 shows Raman spectra of the targets, which has different stoichiometric rates denoted by x. As understand from graph, the most remarkable influence of Al_2O_3 addition to targets is peak shift. Vibrational modes and corresponding peak values are listed in Table 1. For the samples, the spectrum basically consists of four bands. The bands at 140 and 320 cm^{-1} are ascribed to modes involving in plane and c-axis titanium vibration, respectively, while the bands at 239 and 521 cm^{-1} are assigned to oxygen [20]. Moreover, with Al addition, while the peak at 320 cm^{-1} disappears, the peak at about 450 cm^{-1} enhances. The substitution of Ti with Al leads to disappearance of peak at 320 cm^{-1}. Al_2O_3 addition caused peaks to shift left with respect to the pure LLTO peak. Vibrations of Ti and O bonding, and mass difference between Ti and Al have led to these shifts. As a result electrical properties will be affected.

Table 1
Observed modes and attributions for different x-compositions of powder target samples.

Vibrational modes	Raman shift (cm^{-1}) for each composition (x)				
	Pure	x = 0.01	x = 0.05	x = 0.10	x = 0.15
Ti (in-plane)	141.1	145.3	149.8	152.6	161.4
O (3) in-plane	239.8	242.3	242.4	244.4	252.5
Ti (c-axis)	319.4	–	312.8	–	–
O (1,2) c-axis	460.1	454.6	460.0	458.9	466.2
O (3) in-plane	522.6	532.2	530.5	535.4	542.2

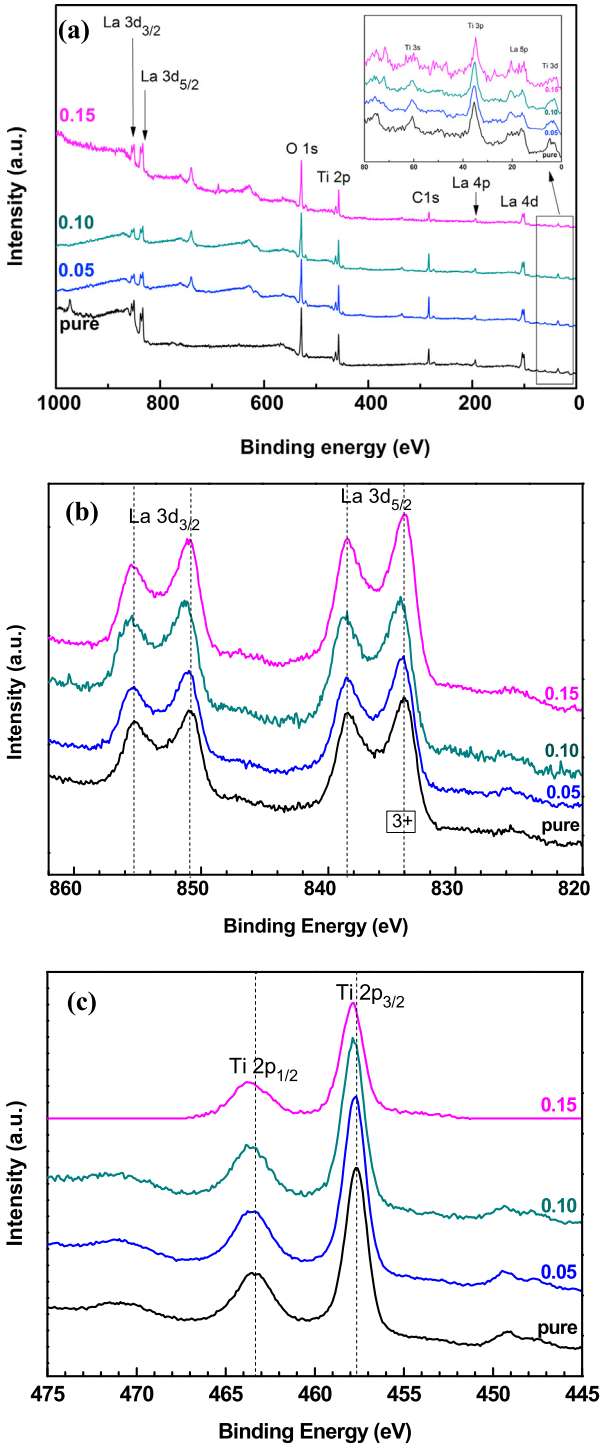

Fig. 5. (a) XPS survey spectra (b) La 3d region (c) Ti 2p region XPS spectra for $Li_{0.5}La_{0.5}TiO_3$ (pure) and $Li_{0.5}La_{0.5}Ti_{1-x}Al_xO_3$ (x = 0.05, 0.10 and 0.15) thin film compositions.

XPS was also used to characterize the chemical nature of thin film electrolytes. In Fig. 5(a) general survey of $Li_{0.5}La_{0.5}Ti_{1-x}Al_xO_3$ thin films with various Al (x) content of pure, 0.05, 0.10, and 0.15 are shown. The XPS spectra consist of peaks assigned to Li 1s, La 4d and 4p, Ti 2p, O 1s and C 1s. C 1s peak at 284.6 eV was used as a reference peak for the calibration. Peaks of La 3d3/2 and La 3d5/2 are shown in Fig. 5(b) for different compositions of thin films but there is no impressive change that can be observed. So, it can be said that binding

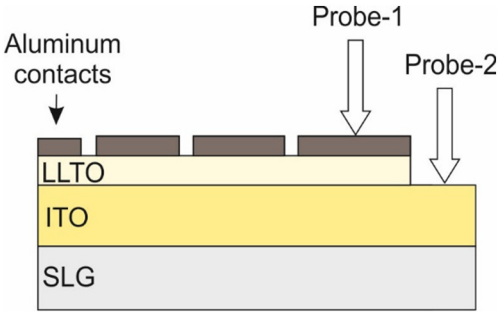

Fig. 6. SLG/ITO/LLTO/Al sandwich structure for AC impedance analyzer measurements.

energies of La 3d is stable against Al addition [21]. However, Ti $2p_{1/2}$ and Ti $2p_{3/2}$ peaks for the $Li_{0.5}La_{0.5}Ti_{1-x}Al_xO_3$ thin film in Fig. 5(c) have shown a slight shift in binding energies toward the higher ones by the increase in Al content. This result corresponds to shortening of Ti−O bond length [22]. The substitution of Ti^{4+} (0.605 Å) with smaller Al^{3+} (0.535 Å) decreases the interatomic Ti−O bond distance and strengthens the bond strength (πTi−O) [23].

Although thin films have amorphous structure, this slight bond shortening of atoms may have a positive effect on Li-ion conduction. So, this microstructural modification may be considered to be beneficial, as it provides electrochemical stability of thin film electrolytes.

3.2. Conductivity evaluation

In Fig. 6, the schematic representation of both contacts on the sample was visualized. Al was evaporated with approximately 100 nm thickness on the upper side of the thin films via the mask with specific diameter size openings. There are 30 different capacitors like structure for one substrate. We have 5 devices from each size of capacitor and we did not see any short circuit.

Ionic conductivity of the thin films was calculated by the chemical impedance analyzer. Using the complex impedance spectra, resistance (Z_R), that cuts the real part of axis, was measured [24]. From real component of resistance, resistivity of the thin films was determined enabling to reach ionic conductivity values of the thin films by the following formula;

$$\sigma = \frac{d}{(R \times A)}$$

where d is the film thickness, R is the electrolyte resistance, and A is the contact area on top of the thin film with different diameter sizes.

In Fig. 7, the complex impedance spectra of as deposited thin film samples with various x compositions were shown. It is observed that the Al addition has positive effect on ionic conductivity, when x is equal to or < 0.10 because x = 0.15 has shown lower conductivity compared to that of pure LLTO. On the other hand, x = 0.01, x = 0.05, and x = 0.10 compositions exhibit higher conductivities. Especially, ionic conductivities for x = 0.01 and x = 0.05 are larger as it can be seen from the Table 2.

So, our results show that the partial substitution of Al^{+3} for Ti^{+4} in $Li_{0.5}La_{0.5}Ti_{1-x}Al_xO_3$ (x = 0.05) improves the Li-ionic conductivity almost about ten times compared to pure LLTO. By opening new conduction paths with decreasing activation energy, higher ionic conductivity at room temperature for the LLTAlO solid state electrolyte is achieved. As the XPS analysis suggests, shortening in Ti−O bond length inside the amorphous structure promotes ionic conduction.

Although LLTAlO thin films still continue to have amorphous structure after annealing, it is observed that anneal treatment has a positive effect on ionic conduction except for the case in x = 0.15 composition. Table 3 shows the ionic conductivities of anneal treated thin film compositions. It can be seen that x = 0.01 composition

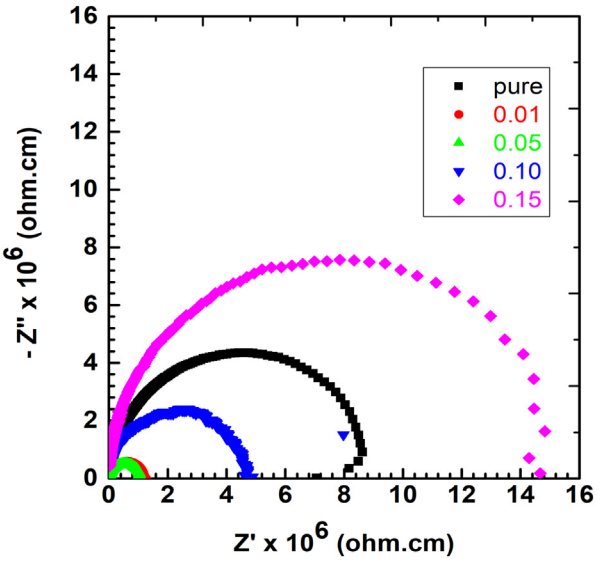

Fig. 7. The complex impedance spectra of as deposited $Li_{0.5}La_{0.5}Ti_{1-x}Al_xO_3$ thin films with different Al contents.

Table 2
Ionic conductivities measured at room temperature from different nominal chemical compositions of thin films.

$Li_{0.5}La_{0.5}Ti_{1-x}Al_xO_3$ (x)	Ionic conductivity (S·cm^{-1}) at RT
0 (pure)	1.42×10^{-7}
0.01	7.96×10^{-7}
0.05	9.68×10^{-7}
0.10	2.16×10^{-7}
0.15	0.68×10^{-7}

annealed at 100 °C has the highest ionic conductivity among all other LLTAlO compositions. Also, SEM image of this sample shows highly connected morphology, which results in higher ionic conduction. Even though there is no trend line with the annealing temperature, it has beneficial effects, because of the stress relaxation inside the thin film structure, on ionic conduction in each case. It is also shown by Bohnke et al., some of the Li ions are captured at the A-cage at the low temperature. When the temperature increase, the number of the long-range moving ions increases. Moreover, at the low temperature bottleneck only in the a and b directions are large enough to let Li ion jumping. At the high temperature, bottlenecks are opened due to the oxygen vibration along the c direction, so Li ions can jump along another direction increasing ion conductivity [25].

3.2.1. Arrhenius plot

In order to determine activation energy for the ion migration from one side to the other, temperature dependent measurements were obtained within the same frequency range (0.1 Hz to 200 kHz) by changing temperature from 298 to 373 K on $Li_{0.5}La_{0.5}Ti_{0.95}Al_{0.01}O_3$ thin film sample, which has the highest ionic conductivity. So, temperature dependence of $Li_{0.5}La_{0.5}Ti_{0.95}Al_{0.05}O_3$ thin film shows non-Arrhenius behavior that can be seen in Fig. 8.

It is observed that after 323 K, slope of the line changes, which means that there is a change in activation energy. In other words, the calculations show that Li-ion conduction mechanism is changed at 323 K (50 °C) that appear in two activation energies as 0.56 eV for T < 323 K, 0.38 eV for T > 323 K. According to the some authors, the diffraction of the line at high temperature because of phase transition inducing a conduction process with two different activation energies [26]. Moreover, the mobility of Li-ions can be enhanced by temperature increment to promote ionic conduction [27,28]. Also some studies show

Table 3
Ionic conductivities of annealed thin film samples for each Al content in LLTO.

Anneal temperature	Conductivity at room temperature (S·cm^{-1}) of each x-composition				
	(x = 0.00)	(x = 0.01)	(x = 0.05)	(x = 0.10)	(x = 0.15)
As deposited	1.42×10^{-7}	7.96×10^{-7}	0.96×10^{-6}	2.16×10^{-7}	6.80×10^{-8}
100 °C	7.92×10^{-9}	2.36×10^{-6}	1.00×10^{-8}	7.15×10^{-7}	very low
200 °C	4.88×10^{-9}	0.85×10^{-7}	1.70×10^{-6}	8.15×10^{-9}	1.97×10^{-8}
300 °C	7.41×10^{-8}	1.03×10^{-7}	1.42×10^{-6}	1.75×10^{-8}	1.24×10^{-8}
400 °C	1.49×10^{-8}	very low	0.12×10^{-6}	4.51×10^{-7}	1.10×10^{-8}

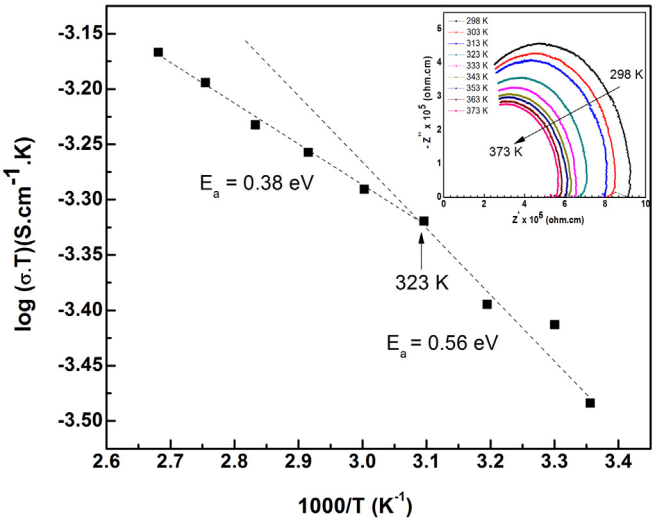

Fig. 8. Arrhenius plots of the conductivity as a function of 1000/T for LLTAlO (x = 0.01) annealed at 100 °C and the inset shows complex impedance curves at each temperature.

that, activation energies lowers at high temperature due to the non-correlation of Li ions. At room temperature the ions jump either in the forward or the backward direction which is highly correlated. With an increasing temperature, the relaxation of lattice becomes faster and the jump of the ions toward to backward decrease causing less correlated motion and then to decrease of the activation energy [25,29]. As a result, it is obvious that LLTAlO thin films are stable in relatively wide temperature range and LLTAlO's ionic conductivity also increases with temperature.

4. Conclusion

Pure and Al doped LLTO targets were prepared successfully by conventional solid state reaction methods from powders. Using these targets, pure and Al doped LLTO thin films were prepared on ITO/SLG by RF magnetron sputtering technique. All the thin films were amorphous. The Al substitution dependence of the ionic conductivity shows that introduction of Al enhances its conductivity. Compared to $Li_{0.5}La_{0.5}TiO_3$ (pure) composition, other Al (x) substituted amounts have given positive effect on conduction except for $Li_{0.5}La_{0.5}Ti_{1-x}Al_xO_3$ (x = 0.15) composition. Highest ionic conductivity is obtained from $Li_{0.5}La_{0.5}Ti_{1-x}Al_xO_3$ (x = 0.01) composition at 100 °C annealing temperature as 2.36×10^{-6} S/cm, which is 20 times higher than that of $Li_{0.5}La_{0.5}TiO_3$ (pure) composition. On the other side, $Li_{0.5}La_{0.5}Ti_{1-x}Al_xO_3$ (x = 0.15) composition has the lowest ionic conduction result. So, it is obvious that over addition of Al_2O_3 decrease the effective pathways for Li-ion conduction. Besides, effect of anneal treatment on thin film samples for every composition is investigated. Although the results do not show a trend-line with the annealing temperature, annealing can be has a positive effect on conduction providing a stress relaxation inside thin film structure caused by the lattice mismatch between the substrate and LLTAlO thin film. Besides, activation energies of best sample were calculated in the range from 298 to 373 K. Li ion conduction mechanism is changing around 323 K. It can be explained by the non-correlation of Li ions at elevated temperatures. Because of its increased ionic conductivity, LLTAlO solid state electrolyte can be used in thin film solid state batteries, RFID, satellites, communication, wearable medical instruments etc.

Acknowledgment

This research was supported by TUBITAK (Scientific and Technical Research Council of Turkey) with project number 114M044. Also, authors would like to thank Applied Quantum Research Center (AQUREC) and Center for Materials Research (CMR) of IZTECH for the research facilities they offer for the current study.

References

[1] J.M. Tarascon, M. Armand, Issues and challenges facing rechargeable lithium batteries, Nature 414 (2001) 359–367.
[2] Y. Wang, Z. Liu, F. Huang, J. Yang, J. Sun, A strategy to improve the overall performance of the lithium ion-conducting solid electrolyte $Li_{0.36}La_{0.56}Y_{0.08}Ti_{0.97}Al_{0.03}O_3$, Eur. J. Inorg. Chem. 5 (2008) 599–602.
[3] Z. Zheng, H. Fang, F. Yang, Z.K. Liu, Y. Wang, Amorphous $LiLaTiO_3$ as solid electrolyte material, J. Electrochem. Soc. 161 (2014) A473–A479.
[4] F. Aguesse, V. Roddatis, J. Roqueta, P. García, D. Pergolesi, J. Santiso, Microstructure and ionic conductivity of LLTO thin films: influence of different substrates and excess lithium in the target, Solid State Ionics 272 (2015) 1–8.
[5] B. Diouf, R. Pode, Potential of lithium-ion batteries in renewable energy, Renew. Energy 76 (2015) 375–380.
[6] E.E. Jay, M.J. Rushton, A. Chroneos, R.W. Grimes, J.A. Kilner, Genetics of superionic conductivity in lithium lanthanum titanates, Phys. Chem. Chem. Phys. 17 (2015) 178–183.
[7] A. Belous, Synthesis and electrophysical properties of novel lithium ion conducting oxides, Solid State Ionics 90 (1996) 193–196.
[8] Y. Inaguma, L. Chen, M. Itoh, T. Nakamura, Candidate compounds with perovskite structure for high lithium ionic conductivity, Solid State Ionics 70–71 (1994) 196–202.
[9] A. Rivera, C. León, J. Santamaría, A. Varez, M.A. Paris, J. Sanz, $Li_{3x}La_{(2/3)-x}TiO_3$ fast ionic conductors correlation between lithium mobility and structure, J. Non-Cryst. Solids 307–310 (2002) 992–998.
[10] A. Morata-Orrantia, S. García-Martín, E. Morán, M.Á. Alario-Franco, A new $La_{2/3}Li_xTi_{1-x}Al_xO_3$ solid solution: structure, microstructure, and Li+ conductivity, Chem. Mater. 14 (2002) 2871–2875.
[11] Z. Zheng, H.Z. Fang, Z.K. Liu, Y. Wang, A fundamental stability study for amorphous $LiLaTiO_3$ solid electrolyte, J. Electrochem. Soc. 162 (2015) A244–A248.
[12] K.K. Bharathi, H. Tan, S. Takeuchi, L. Meshi, H. Shen, J. Shin, S. Takeuchi, L.A. Bendersky, Effect of oxygen pressure on structure and ionic conductivity of epitaxial $Li_{0.33}La_{0.55}TiO_3$ solid electrolyte thin films produced by pulsed laser deposition, RSC Adv. 6 (2016) 61974–61983.
[13] A. Morata-Orrantia, S. Garcıa-Martin, M.A. Alario-Franco, Optimization of Lithium conductivity in La/Li titanates, Chem. Mater. 15 (2003) 3991–3995.
[14] B.S. Youmbi, S. Zékeng, S. Domngang, F. Calvayrac, A. Bulou, An ab initio molecular dynamics study of ionic conductivity in hexagonal lithium lanthanum titanate oxide $La_{0.5}Li_{0.5}TiO_3$, Ionics 18 (2012) 371–377.
[15] O. Tuna, Y. Selamet, G. Aygun, L. Ozyuzer, High quality ITO thin films grown by DC and RF sputtering without oxygen, J. Phys. D. Appl. Phys. 43 (2010) 55402.
[16] H. Koseoglu, F. Turkoglu, M. Kurt, M.D. Yaman, F.G. Akca, G. Aygun, L. Ozyuzer, Improvement of optical and electrical properties of ITO thin films by electro-annealing, Vacuum 120 (2015) 8–13.
[17] S. Ulusoy, Ionic Conductivity of Li0.5La0.5Ti1 − xAlxO3 Electrolyte Layer for Thin Film Batteries (A Thesis Submitted to Izmir Institute of Technology), (2016).
[18] Y. Xiong, H. Tao, J. Zhao, H. Cheng, X. Zhao, Effects of annealing temperature on structure and opt-electric properties of ion-conducting LLTO thin films prepared by RF magnetron sputtering, J. Alloys Compd. 509 (2011) 1910–1914.

[19] K.P. Abhilash, P. Christopher Selvin, B. Nalini, K. Somasundaram, P. Sivaraj, A. Chandra Bose, Study of the temperature dependent transport properties in nanocrystalline lithium lanthanum titanate for lithium ion batteries, J. Phys. Chem. Solids 91 (2016) 114–121.
[20] B. Antoniassi, A.H. González, S.L. Fernandes, C.F. Graeff, Microstructural and electrochemical study of $La_{0.5}Li_{0.5}TiO_3$, Mater. Chem. Phys. 127 (2011) 51–55.
[21] R.J. Chen, W. Liang, H.Q. Zhang, F. Wu, L. Li, Preparation and performance of novel LLTO thin film electrolytes for thin film lithium batteries, Chin. Sci. Bull. 57 (2012) 4199–4204.
[22] S. Wenzel, T. Leichtweiss, D. Krüger, J. Sann, J. Janek, Interphase formation on lithium solid electrolytes - an in situ approach to study interfacial reactions by photoelectron spectroscopy, Solid State Ionics 278 (2015) 98–105.
[23] L.X. He, H.I. Yoo, Effects of B-site ion (M) substitution on the ionic conductivity of $(Li_{3x}La_{2/3-x})_{1+y/2}$ $(M_yTi_{1-y})O_3$ (M = Al, Cr), Electrochim. Acta 48 (2003) 1357–1366.
[24] R. Huggins, Simple method to determine electronic and ionic components of the conductivity in mixed conductors a review, Ionics 8 (2002) 300–313.
[25] O. Bohnke, The fast lithium-ion conducting oxides $Li_{3x}La_{2/3-x}TiO_3$ from fundamentals to application, Solid State Ionics 179 (2008) 9–15.
[26] S. Stramare, V. Thangadurai, W. Weppner, Lithium lanthanum titanates: a review, Chem. Mater. 15 (2003) 3974–3990.
[27] S. Salkus, E. Kazakevicius, A. Kezionis, A.F. Orliukas, J.C. Badot, O. Bohnke, Determination of the non-Arhenius behaviour of bulk conductivity of fast ionic conductors LLTO at high temperature, Solid State Ionics 188 (2011) 69–72.
[28] A. Rivera, J. Santamaria, C. Leon, T. Blochowicz, C. Gainaru, E.A. Rossler, Temperature dependence of the ionic conductivity in Li3xLa2/3 − xTiO3: Arrhenius versus non-Arrhenius, Appl. Phys. Lett. 82 (2003) 2425–2427.
[29] K.L. Ngai, A.K. Rizos, Parameterless explanation of the non-Arrhenius conductivity in glassy fast ionic conductors, Phys. Rev. Lett. 76 (1996) 1296–1299.